A Study of Ferroresonance

&

Mitigation Techniques

April 28th, 2013

Beau Baldwin, Salil Sabade, Shailesh Joshi

Michigan Technological University

Executive Summary

An electric circuit consisting of a non – linear inductance connected in series with a capacitance and a voltage source involving low losses, in which an oscillatory phenomenon is observed, is said to be a ferroresonant circuit. Ferroresonance is commonly seen in transformers as they have non – linear magnetic characteristics and sometimes operate in no – load conditions. The capacitance in this case can be due to the mutual coupling between the windings, underground cables or capacitor banks et al.

Generally, ferroresonance is observed after any transient disturbance like lightning strikes, switching operations, faults etc. The occurrence of ferroresonance is very dangerous for the system and it will propagate itself as sustained overvoltages and overcurrent's laden with harmonics. Over the past couple of decades, the power grid has seen a drastic change in the type of loads it has to support, increased use of underground cables, amorphous core transformers, and numerous single – phase switching operations has resulted in rise of number of failures occurring due to ferroresonance.

For this study, a medium voltage transmission system was simulated consisting of an underground cable energizing a 3– phase transformer under light load conditions. This system was developed using Alternate Transients Program (ATP) part of the Electromagnetic Transients Program (EMTP) package. The transformer was subjected to single phase switching, resulting in the formation of a series LC combination prone to ferroresonance. The waveforms obtained were analyzed and used to design damping circuits and harmonic filters which have been implemented to mitigate ferroresonance in the system.

The simulated ferroresonance phenomenon was suppressed using an air core inductor bank connected to the secondary of the transformer as well as a LC '*T*' type Butterworth filter. The result was a reduced harmonic content and dampened event when compared to a non-filtered event. Thus, it is advised to have a suppression circuit connected to the system. A few commercially available solutions have been illustrated and the effectiveness of the measures to mitigate the problem has been scrutinized.

Table of Contents

Figure List

Introduction

Transient events generally occur due to switching actions in the system and also depend on system parameters like resistance, inductance and capacitance of transmission line, transformer load condition, capacitive and inductive shunt reactors etc. Due to these parameters and eventually the stacking of various capacitive and inductive components into the system, the frequency range of transient phenomena can vary from DC to several MHz [1]. Now, depending on the frequency range, types of transient events are divided into high and low frequency transients which helps to understand and communicate the effects of transients in a simple way.

Ferroresonance would occur in the system when, depending on the circuit configuration and large number of different sources of capacitance in the network combined with certain sequence of switching events occur. To put in simple words, term *'ferroresonance'* means the resonance between the network parameters with ferromagnetic material and specifically with the presence of transformers when operating at no-load condition [3].

The term 'Ferroresonance' was first coined by Boucherot when he observed this phenomenon in 1920. Now – a – days, the term ferroresonance is interpreted as not just a jump in variation in the fundamental frequency state but also the various sub types, **sub – harmonic, quasi – periodic and even chaotic** oscillations in circuits consisting non – linear inductance. Electric networks are made up of a large number of saturable inductances like power transformers, voltage transformers (VT), shunt reactors as well as capacitors like cables, capacitor voltage transformers, series or shunt capacitor banks et al which are the components due to which various types of ferroresonance could occur [4].

This phenomenon is very dangerous to the system since more than one steady state can be observed and the normal steady state response of a system could leap to a ferroresonant steady state but characterized by large overvoltages and harmonics. A few serious consequences of ferroresonance observed previously are untimely tripping of protection devices, permanent damage to transformers, and drastic increase in power losses causing large dissipation of heat.

The vision for this project is to analyze various cases of ferroresonance occurring in power systems, model and simulate a system showcasing it and trying to find various mitigation techniques to overcome this problem. The best action against ferroresonance is not to let it occur in the first place by changing initial design or conditions of the system and also having preset mitigation actions in place to suppress it.

Background/Literature Survey

Linear resonance will occur in a circuit comprising of series connected resistor, inductor and capacitor as shown in figure 1 and when the source is tuned to the natural frequency of the circuit. The capacitive and inductive reactances of the circuit are identical at the resonance frequency (F_R) and is described as,

$$F_R = \frac{1}{2\pi\sqrt{L*C}} \text{ Hz} \qquad \ldots. (1)$$

This can be controlled by using frequency control strategies or by using pure resistance which dissipates power as heat. This response from the system is expected and predictive which can be controlled since it is a linear circuit.

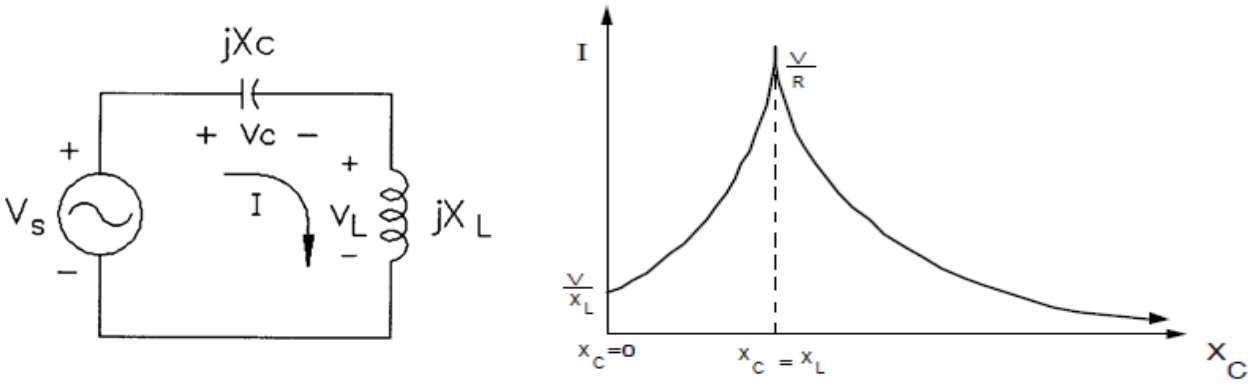

Figure 1: Series RLC Circuit

However in non – linear circuit, i.e., a circuit comprising of resistance , capacitance and a non – linear inductor, ferroresonance occurs at a given frequency when one of the saturated core inductances matches with the capacitance of the network. The final effect is that there are several steady state overvoltages and overcurrents present. Figure 2 shows a non – linear circuit capable of ferroresonance.

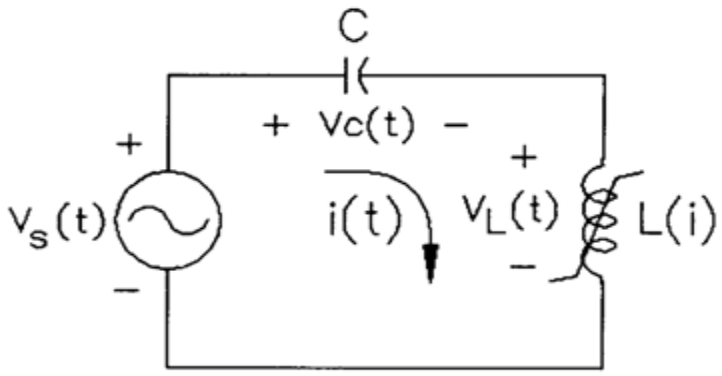

Figure 2; Non – linear LC Circuit in Which Ferroresonance is Possible

In a non – linear LC circuit as shown above in figure 2, the voltage across the inductance (V_L) depends on the frequency (ω) and the current through a function, f(I) and can be represented as,

$$V_L = \omega\, f(I) \qquad \text{…….. (1)}$$

Now, the voltage across the capacitor is given equation 2. The minus sign indicates that the capacitive voltage (V_C) is in anti – phase with inductive voltage and lags the current by 90^0. The total voltage will be given as shown in equation 3.

$$V_C = -\frac{I}{\omega C} \qquad \text{…….. (2)}$$

$$V_L = Vs + \frac{I}{\omega C} \qquad \text{……. (3)}$$

From equation 3 it is clear that inductive voltage has a fixed component and a variable component. However, if the value of X_L varies assuming it is an iron core transformer, then the possibility of X_C to match X_L rises considerably. Figure 3 shows the solution to the linear circuit. The intersection between the inductive reactance X_L line and thee capacitive reactance X_C line yields the current in the circuit and the voltage across the inductor (V_L). However, when X_L is no longer linear, i.e., it is a saturable inductor, the reactance (X_L) cannot be shown as a straight line. The graphical result for non – linear circuit is shown in figure 4 [5].

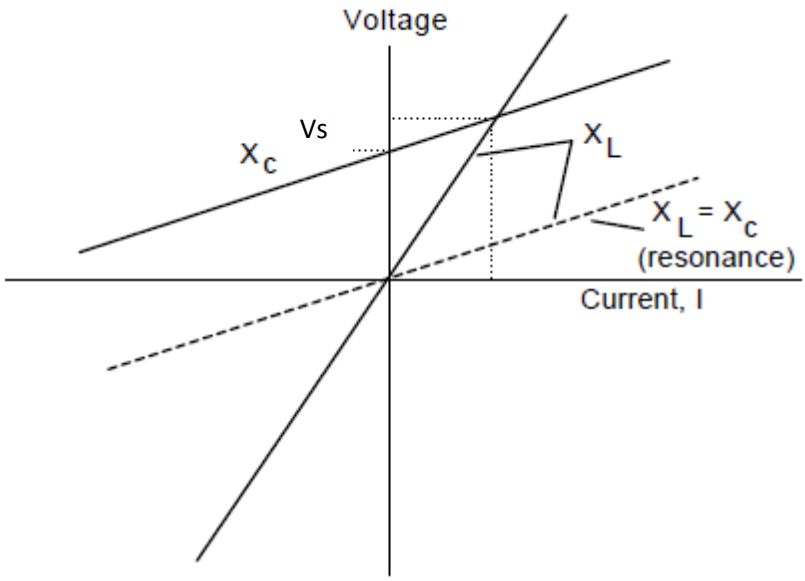

Figure 3: Graphical Solution for Linear Circuit

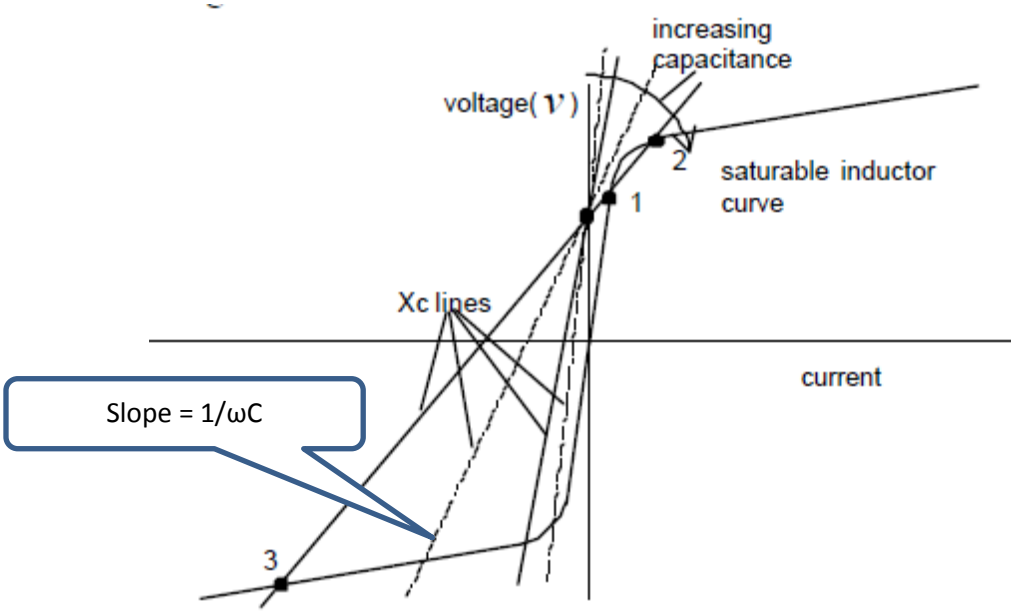

Figure 4: Graphical Solution for Non – Linear Circuit

From figure 4 it can be seen that there could upto three intersection points between the capacitive reactance (X_C) and inductive reactance (X_L) characteristics. Intersection 2 is an unstable operating point and the solution will not remain in steady state, but it could pass through this point during a transient occurrence. For intersection 3 there will be both high voltages and high currents. For small capacitances, the X_C line is quite steep which would result only in one intersection in the third quadrant. The capacitive reactance is larger than inductive reactance which would result in a

leading current with higher than normal voltages across capacitor. As the capacitance increases, from graph it can be seen that more intersections can be achieved. Now for intersection 1, which is basically an inductive solution with lagging current and little voltage across the capacitor, the voltage across capacitor is a LG voltage on the cable. In case a slight increase in voltage occurs, the X_C line would shift upward which would eliminate intersection 1. This will cause the voltage to keep jumping between 1 and 3. This will cause the voltage and current appear varying randomly and unpredictably [5].

Papers published by *Escudero, Redfern, Dudurych* [6] mentions a ferroresonance incident experienced on a newly commissioned 400 kV substation in Ireland. The circuit of this substation is as shown in figure 4. The authors mention that the cause of the phenomenon was due to the switching events that have been carried out for commissioning of the new 400 kV substation which forced two single – phase voltage transformers (VTs) in a sustained ferroresonant state.

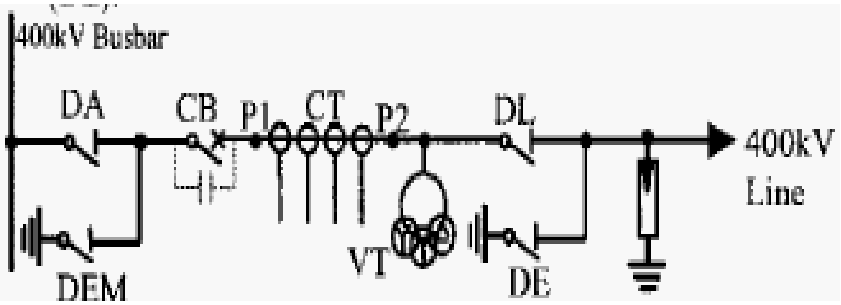

Figure 5: Circuit Diagram of 400 kV Substation

The commissioning of the system was conducted such that the VTs from the Bus-Bars were energized by disconnecting the line disconnector (DL) and then de-energized the VTs by opening the circuit breaker (CB). The effects after the switching events reconfigured the circuit into ferroresonance state involving the interaction between the circuit breaker's grading capacitor and the two voltage transformers.

A paper published by Jacobson [7 8], investigated a severely damaged wound potential transformer caused by a sustained fundamental ferroresonance. The failure observed was thought to be due to excessive current flow in the primary winding because of sustained ferroresonance between the CB grading capacitance and non – linear magnetizing inductance of the voltage transformer.

According to the authors, the complete bus was disconnected in order to have the equipment replaced that was damaged due to the ferroresonant effect. The switching that occurred at the station caused the bus to which VTs are connected to de-energize and then connected VTs through the grading capacitor of the circuit breaker to other bus which is energized. This caused the prolonged

ferroresonance condition thereby resulting in equipment failure and causing physical damage to VT. Since the occurrence of this incident all the wound VTs were replaced with capacitor VTs and 200Ω loading resistors were installed on the 4.16 kV secondary bus of service transformers SST1 and SST2 as shown in figure 5. The manual de-energizing operating procedure need not be used anymore since wound VTs are not used and loading resistors have been introduced.

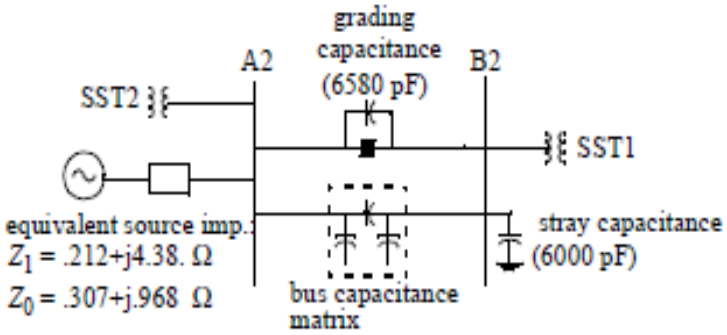

Figure 6: One Line Diagram after Installation of Capacitor Bank and Loading Resistors

As has been seen until now, the scenarios under which ferroresonance can occur are limitless and this could be due to various core and winding configurations in the transformer [9]. There are various reasons which can initiate ferroresonance like loss of grounding systems, switching or may be actuation of fuses. Figures 6a and 6b show the configurations that may lead to ferroresonance. The configuration could either be star or delta connected and in unbalanced conditions is good enough to cause ferroresonance combined with single – phase switching, unloaded transformer operation, etc.

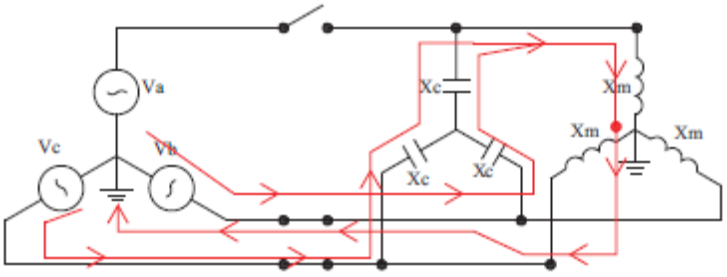

Figure 7: Single – Phase Switching with Primary Connected as Grounded – Wye

Each phase of the transformer is represented by magnetizing reactance (X_M). Now when a phase is opened and if the capacitor bank or say transformer contains a grounded neutral, a series path through the capacitance and the magnetizing reactance would be created as can be seen in the figures marked by red lines which could create favorable conditions for ferroresonance. However, if both the neutrals are grounded (i.e. of capacitance and inductance) the possibility of ferroresonance is almost eliminated since there cannot be a series path between the capacitance and inductance. This is also applicable to delta connection.

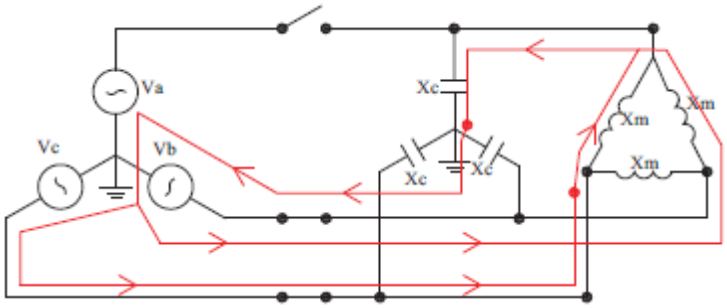

Figure 8: Single – Phase Switching with Primary Connected as Delta

To understand and study ferroresonance in a circuit, various methods need to be applied. Now depending on the transformer core, it is still possible to observe ferroresonance even if a direct series path between capacitance and inductance does not exist. This is possible since some three phase cores have direct coupling among the phases causing induced voltage into the open phase of the transformer. So, some methods were suggested to study this phenomenon and are listed below.

1. *Laboratory and field tests:* This can give the most realistic observations but there is limit to the number of tests that can be performed since it can cause permanent damage to the transformer.
2. *Mathematical and Analytical methods:* This method provides considerable flexibility in most cases but it limits analysis to single phase cases since three phase cases pose complex difficulties.
3. *Digital Simulation Tools :* The most suitable option is to use simulation tools like MATLAB, ATP, etc. which allow high level of flexibility, increased number of scenarios and can accommodate three phase systems.

From the above discussion it is evident that simulation tools will be used to study this phenomenon and hence it is important to understand how they work and the actual models will have to be developed to resemble real equipment. For example, the transformer response is based on the magnetic coupling between its windings and the core saturation (depends on the material) when a low or medium frequency transient condition is observed. In case of high frequency transients, the response of transformer is influenced by stray capacitances and capacitances among windings.

It is very complicated to represent a transformer since it has a very wide range of winding and core configurations and also certain parameters are non – linear and frequency dependent. It is important to get the transformer right to analyze the phenomenon, hence the model representing the transformer can be split into two parts, first is the windings section (considered linear) and the second

would be the core (considered non – linear) and both are frequency dependent. For ferroresonance it is important to focus on the core section since the ferroresonance effect originates in core.

A hybrid model of transformer has been used system. The model supports three-phase, two and three winding transformers, autotransformers, and wye and delta couplings. Although it is an extremely powerful model, it is rarely utilized due to its complexity and the quantity of data that needs to be informed for it to be properly implemented in the simulation. The necessary information for representing the transformer with this model may be obtained from three different ways, design project (geometry, and the type of material of the windings and core), manufacturer tests and typical data based on nominal power and voltage.

Implementation of model and ferroresonance modes

The primary objective is to simulate a case of ferroresonance in order to retrieve data results from it and use these results to determine a way to either mitigate the effects of the event or dampen them. The system simulated was a medium voltage transmission / distribution system. The simulation tool utilized was the Alternate Transients Program (ATP) portion of the EMTP package. Since most cases of ferroresonance encountered at distribution levels had pad – mounted transformers with delta-connected primary circuits energized by long lengths of underground cables, it was decided to simulate a similar system. [11, 12, 13].

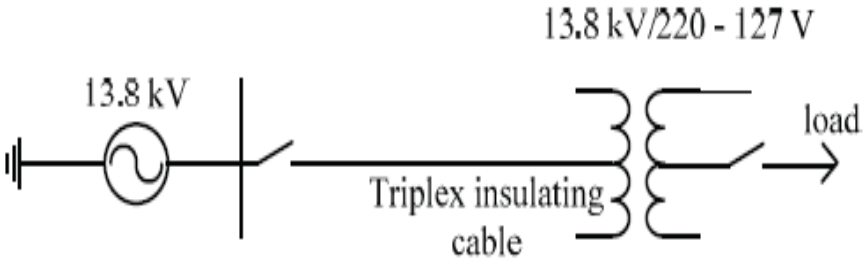

Figure 9: Single Line Diagram of the Ungrounded Circuit

The above system consists of a 3 –phase source operating at 13.8 kV connected in series with a circuit breaker to an underground cable feeding a 75 kVA distribution transformer. This transformer then powers a balanced three phase resistive load. The physical data of the entire system can be found in the attached appendix A. Below is the ATP model used to simulate the above circuit.

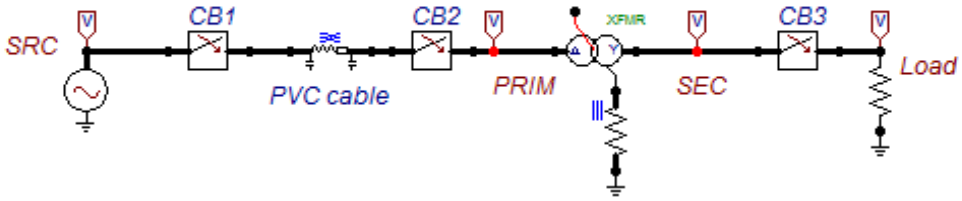

Figure 10: Modeled ATP System

Transformer Characteristics

As covered in the background, the most critical aspects regarding the study of ferroresonance is the modeling of the transformer's core characteristics. To then accurately represent a transformer requires all of the parameters of the transformer to be known. This includes its saturation (core) characteristics as well as the winding characteristics.

There are three non-linear magnetic effects introduced by the saturation of iron cores:

1. Saturation
2. Hysteresis
3. Eddy Currents

For most simulation cases the Hysteresis and Eddy currents are approximated using a non-linear resistor representation in the core-losses. The saturation behavior i.e. magnetizing circuit of the transformer is represented by a non-linear inductor based on the B-H curve or open circuit test results. For understanding certain aspects of core modeling, simulations were carried out on a 120-240 V dry type transformer, modeled in an ATP simulation provided by Dr. Bruce Mork. [9]

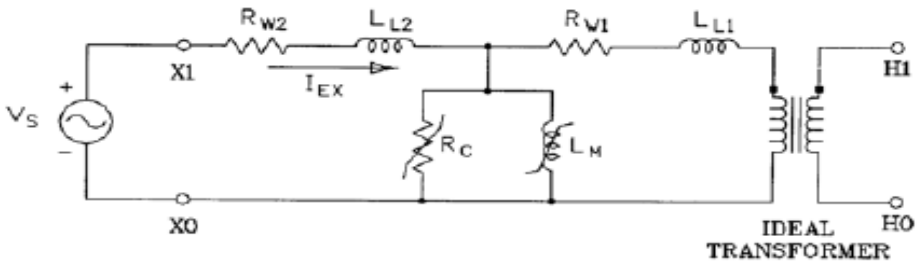

Figure 11: Non-Ideal Transformer

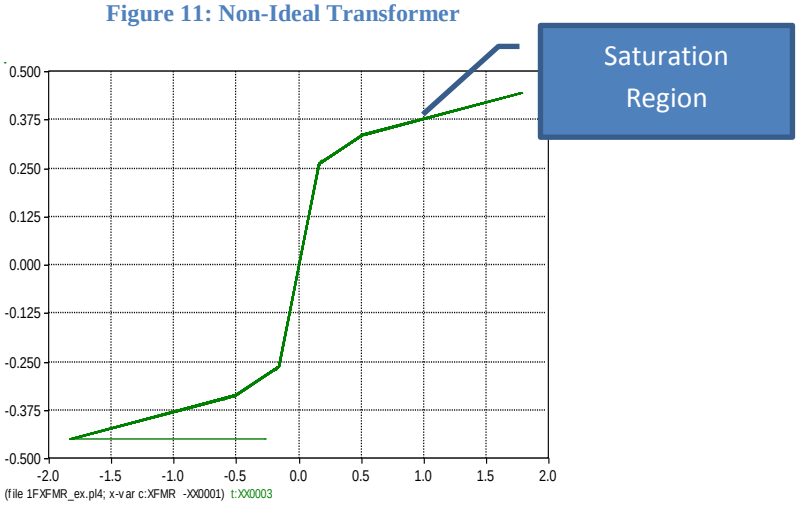

Figure 12: Simulated Saturation Curve

The non-linear inductor models (type 93, 98, 96) available in ATP were scrutinized and their internal piece-wise linear representation of the flux linkage vs. magnetizing current was studied. The non-linearity of the inductor can be represented by the equation:

$$I_{mag} = a.\lambda + b.\lambda^{n} \quad \ldots\ldots\ldots (4)$$

Where,

I_{mag}: Magnetizing current (Amps)

λ: Flux linkage (Wb*Turns - Tesla)

In the linear region, the saturation characteristics can be represented by the first part of equation (4). The addition of the latter part comes into picture when representing the non-linear nature of iron-core inductor; the higher the degree of saturation, the higher the order of magnitude of the non-linearity variable (n). Discussion of the non-linearity modeling considerations falls outside the scope of the current project thus this subject is just touched upon here. Much deeper insights into this characteristic are covered in ref [7, 15].

Modes of Ferroresonance:

Fundamental Mode :

The periodic response has the same period (T) as the system and the frequency spectrum of the signals consists of fundamental frequency component as the dominant one followed by decreasing contents of 3^{rd}, 5^{th}, 7^{th} and n^{th} odd harmonic. Figure 13 show the periodic signal and a frequency spectrum plot which traces the fundamental mode of ferroresonance in a system [ref #].

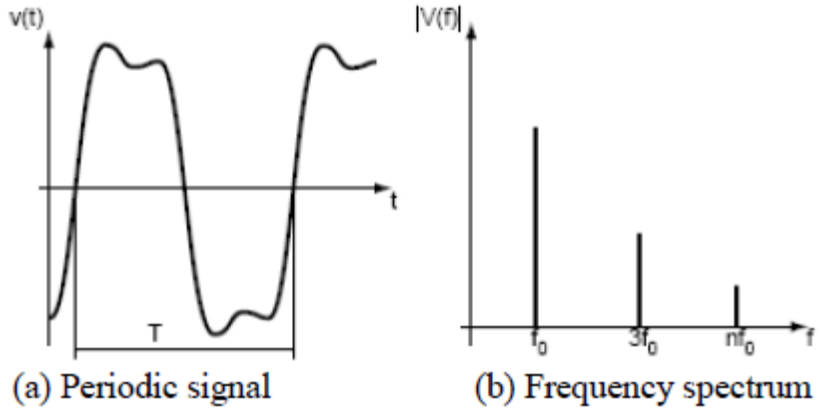

Figure 13 : Fundamental mode of ferroresonance signal

Sub – harmonic Mode :

This type of ferroresonance signals has a period which is multiple of the source period (nT). The fundamental mode of ferroresonance is normally called the First Period (i.e. f_0/1 Hz) ferroresonance and a ferroresonance with a sub-multiple of the power system frequency is called N – Period (i.e. f_0/n Hz) ferroresonance. Figure 14 shows the sub – harmonic mode of ferroresonance signal.

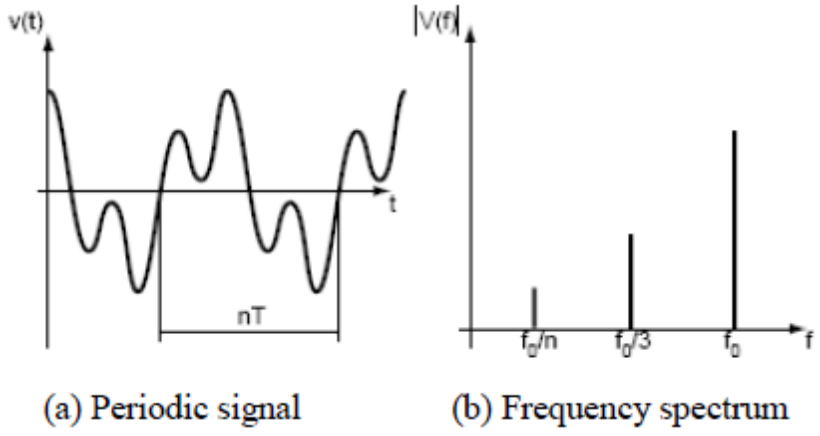

Figure 14 : Sub - Harmonic mode of ferroresonance signal

Quasi – Periodic Mode :

This kind of ferroresonant signal is not periodic. The frequency contents in the signal are discontinuous in the frequency spectrum and whose frequencies are defined as: $nf_1 + mf_2$ (where n and m are integers and f_1/f_2 an irrational real number). Figure 15 shows the quasi – periodic waveform.

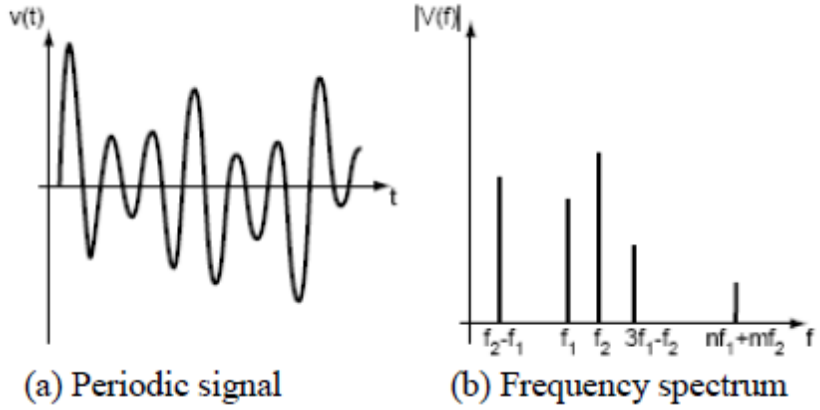

Figure 15 : Quasi - periodic waveform

Chaotic Mode:

This mode has a signal exhibiting non-periodic behavior with a continuous frequency spectrum which basically it means it is not cancelled for any value of frequency. Figure 16 shows the chaotic mode of the ferroresonant signal.

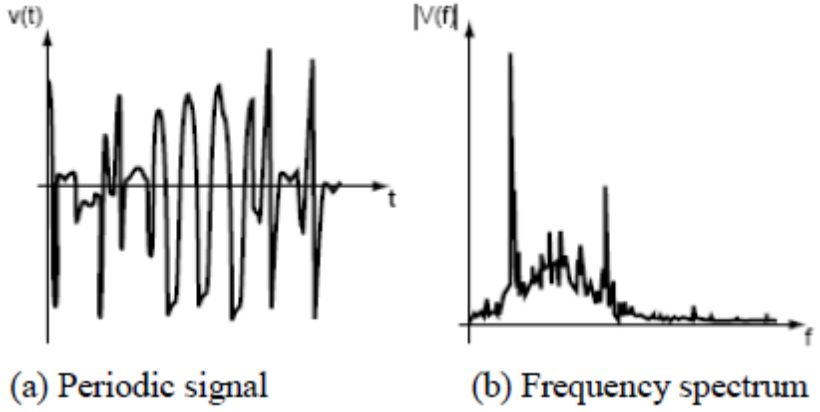

Figure 16 : Chaotic mode of ferroresonance

Simulation

The simulations were performed using ATP's 3-phase Hybrid transformer model [19]. This model is then subjected to single phase switching. By keeping phases B & C energized, phase A was opened at 20 ms. The waveform below was obtained from this simulation and was verified against those declared in ref [9].

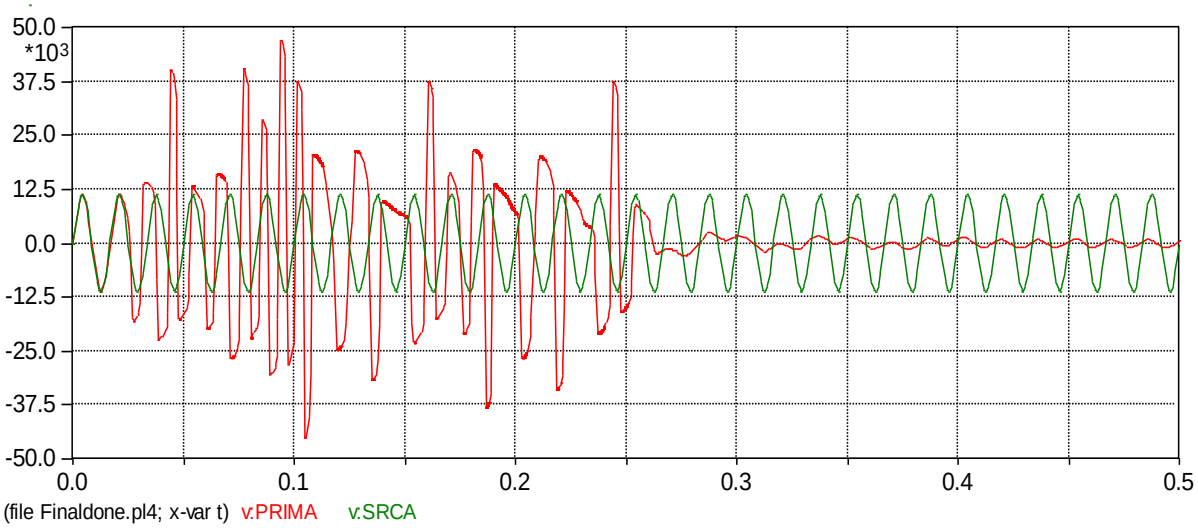

Figure 17: Simulated A Phase Voltage

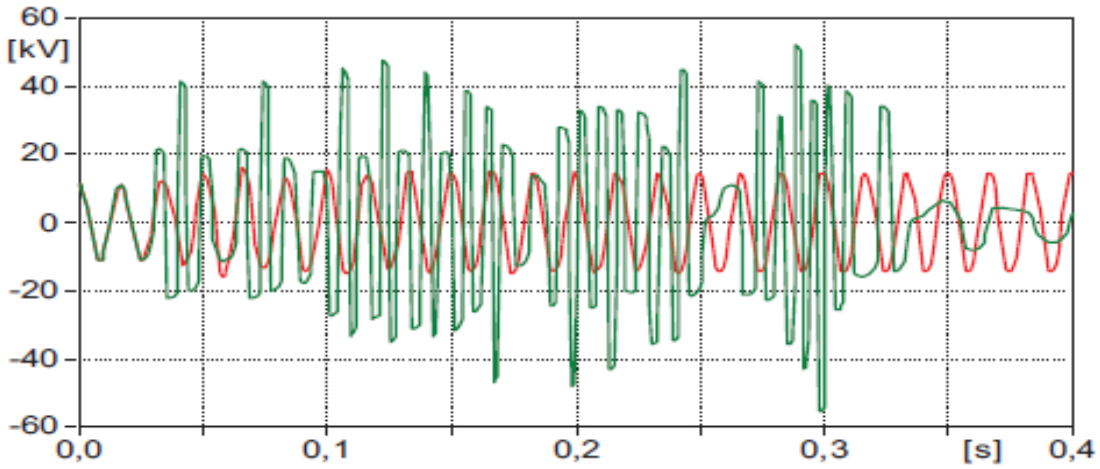

Figure 18: Benchmark A Phase Voltage

The duration and peak of the two waveforms might differ due to some of the assumptions regarding mutual capacitive coupling values between windings and some cable parameters. It can be seen that the voltage waveforms are highly distorted with harmonics and peak values approaching four per

unit. The FFT analysis of the waveform shows the high frequency results shown in the voltage waveform above.

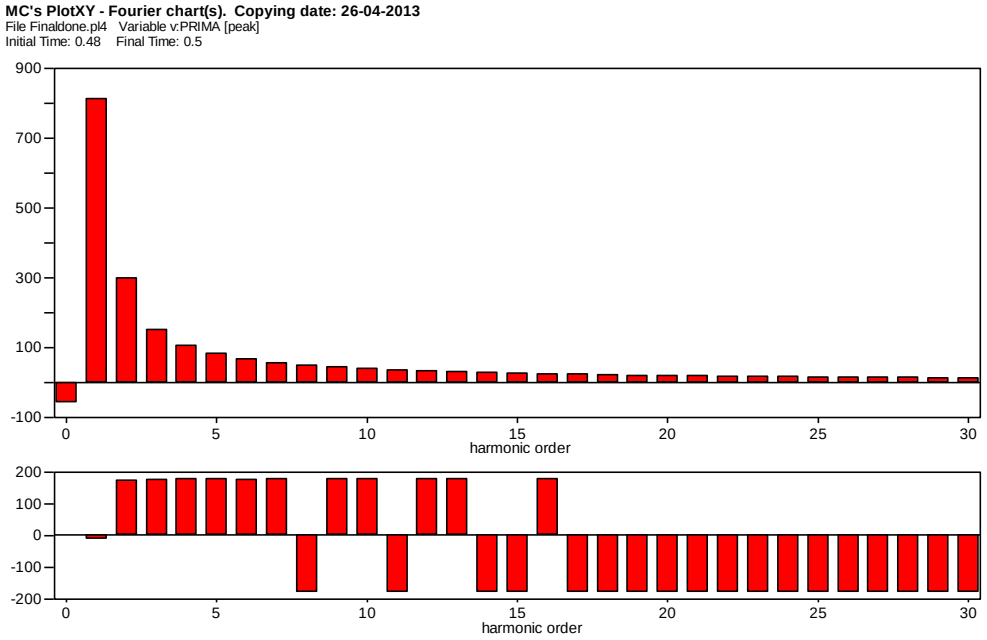

Figure 19: Fourier Analysis of Simulation

The highest magnitude harmonic, as expected, is the fundamental harmonic component. The frequency response pattern corresponds to the 1st mode of ferroresonance. The numerical data of the harmonic content is attached in the APPENDIX.

The waveforms of the two energized phases (B& C) are unaffected .

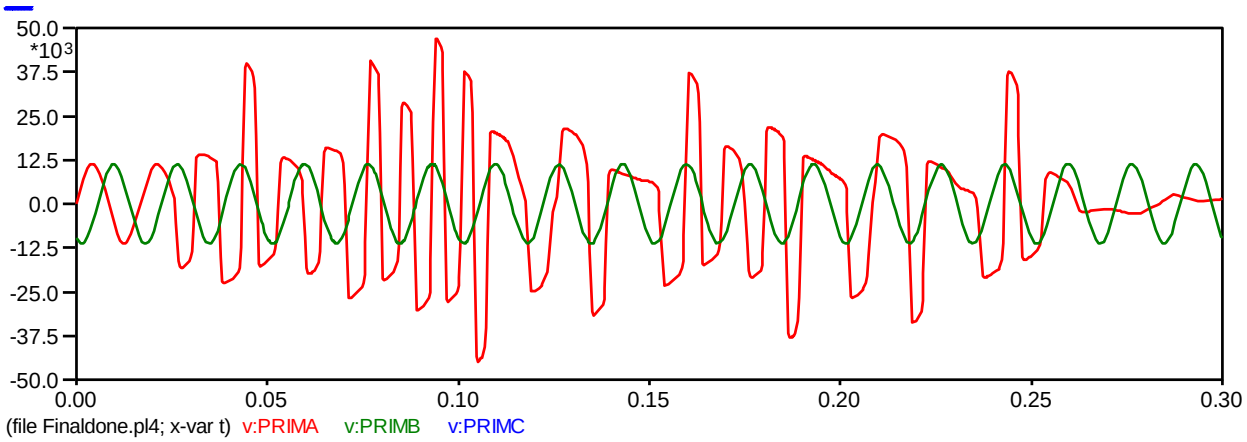

Figure 20: Voltage waveforms of other two phases, the L-L voltage is 13.8 kV rms.

Suppression Techniques and Modeling

With the varying techniques to mitigate ferroresonance a few new possibilities were modeled to see their effectiveness. This includes a "T" style LC band – pass filter and ideal Butterworth. Through the simulation using ATP a series of voltages with respect to time were gathered during the ferroresonant phenomena. This series of data collected consisted of 100001 points of data from 0 to 0.5 seconds or 30 cycles. Using this data is was possible to then simulate this event in various simulation packages. In this case, MATLAB Simulink was utilized for its flexibility and ATP provided a current output of the event as seen below in figure 20.

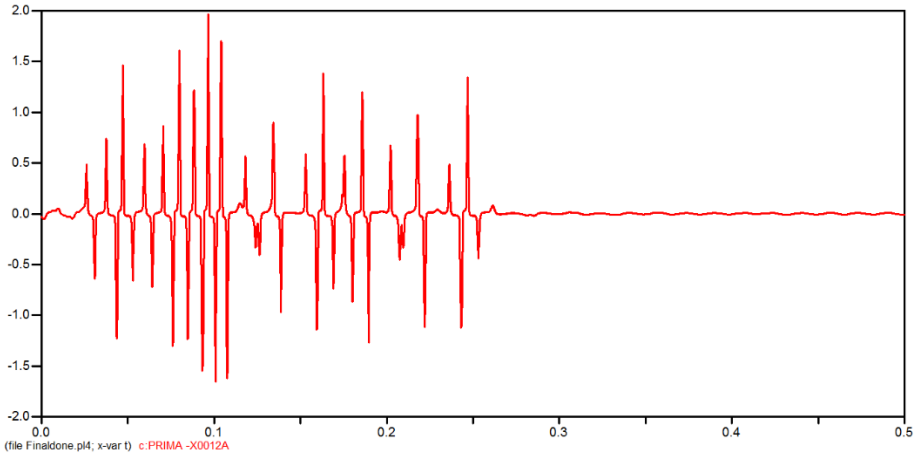

Figure 21: Current Waveform w/out Capacitors

As can be seen the current peaks at about 2A. It was then decided that due to this a very rudimentary resistance could be calculated as a virtual load for the filter simulations. Using the line to neutral line voltage of the system as well as this current a resistance of 3983.7169 Ω was chosen for initial simulations. This value was then determined to be invalid as the calculation of the event should have used the voltage during the event not the line voltage. It was because of this that a newly calculated value of 2350 Ω was utilized for all future simulations.

LC "T" style Butterworth Filter Simulation

The first preliminary filter was designed to suppress harmonics seen in the voltage output from the ATP simulation, specifically the 3rd, 5th and 7th. The goal was to also suppress any DC component that could cause any number of problems for a transformer if left unchecked for extended periods. The simplest choice was a LC filter due to its inherent lossless design. With negligible real

power burning components (resistance) heat should not be a major factor. The components sizing was done using the equation below:

$$\omega = \frac{1}{\sqrt{L * C}}$$

With the desired fundamental being ω.

The simulated system is on the US grid operating at 60Hz / ~377 radians per second. As can be seen by this equation the values of capacitance and inductance are linearly related. If you increase one by a factor of 2 you decrease the other the same factor. The value of a high voltage capacitor is typically very small. With capacitance typically being measured by the kVAR at this voltage level a kVAR of 175 was chosen to represent a small order of capacitance while still being obtainable. A 175kVAR capacitor at 13.8kV would mean a capacitance of ~2.44µF. With such a small capacitance value it inherently means that a high value of inductance was required. Using the equation above it was determined that a ~2.89H inductor would be required. Utilizing different variations of capacitance and inductance does not affect the circuit only the manufacturability of a product capable of acting as such. It was decided to continue simulation with these values.

Multisim LC Filter

The initial design simulation was verified in a rapid testing simulation package by the name of Multisim by National Instruments. This software allows for quick implementation of physical components and simple graphical analysis. The figure below shows the layout in Multisim of the LC filter implemented.

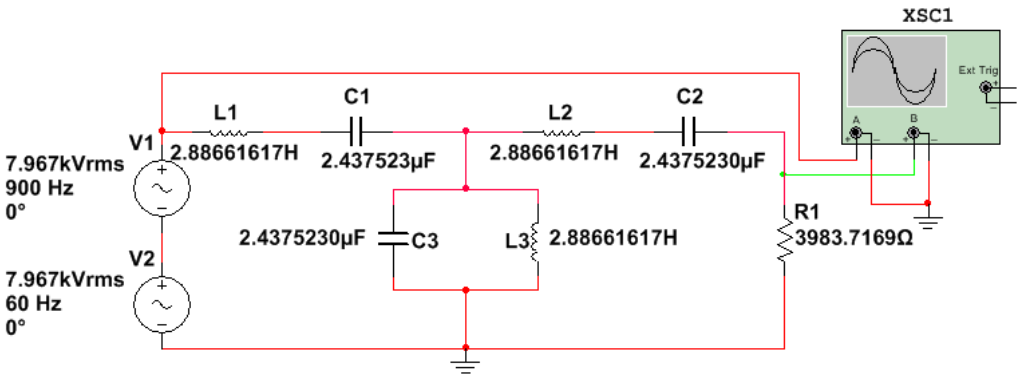

Figure 22: Multisim LC Filter Model

The voltage source used was a 60Hz line voltage (L-N) source in series with a 900Hz source with the same voltage. This creates a 900Hz wave over the fundamental 60Hz. The goal of this simulation was to see if the filter would act as expected. The result of the simulation is shown below.

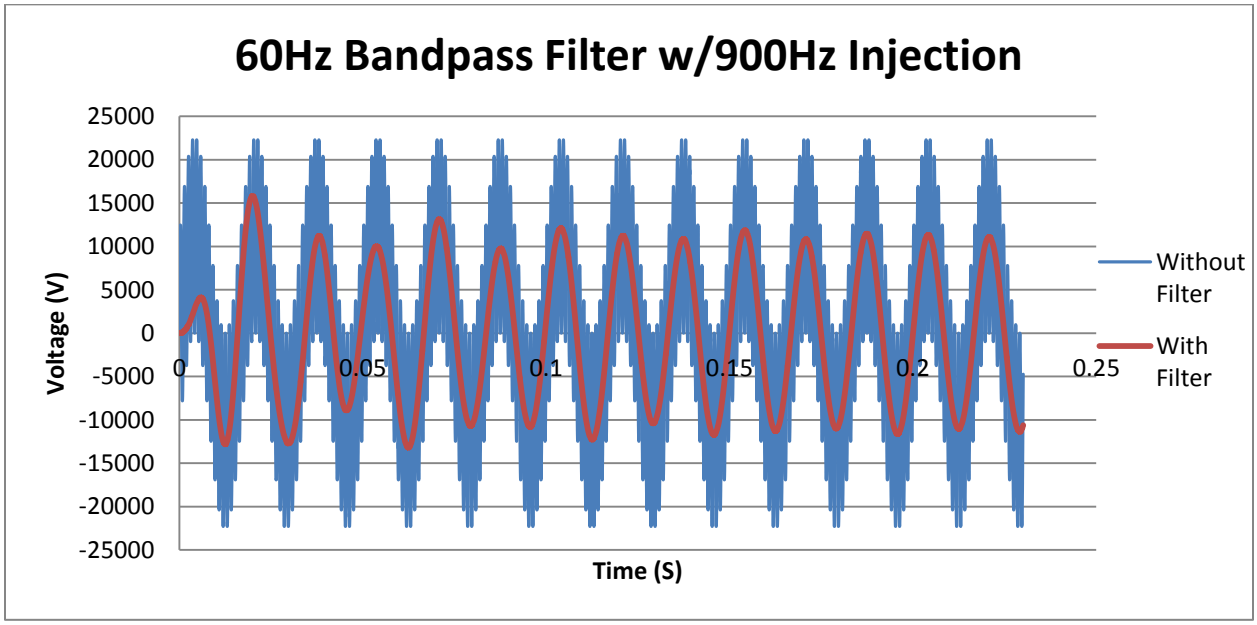

Figure 23: Multisim LC Simulation Result

As can be seen by the above graph the filter significantly suppressed the noise /harmonic present on the line. This simulation showed that the filter could possibly be used to suppress the harmonics present during the ferroresonant event. It was decided to then take this filter to the next level and simulate it with Matlab Simulink.

Matlab Simulink LC Filter

This software is a bit more complex but with the complexity comes adjustability. The goal of using this software was to be able to implement the 100001 samples retrieved from the ATP simulation and see if the same circuit could suppress it. This voltage is much less structured than the 900Hz harmonic simulated in Multisim. The circuit below is the layout of the simscape model.

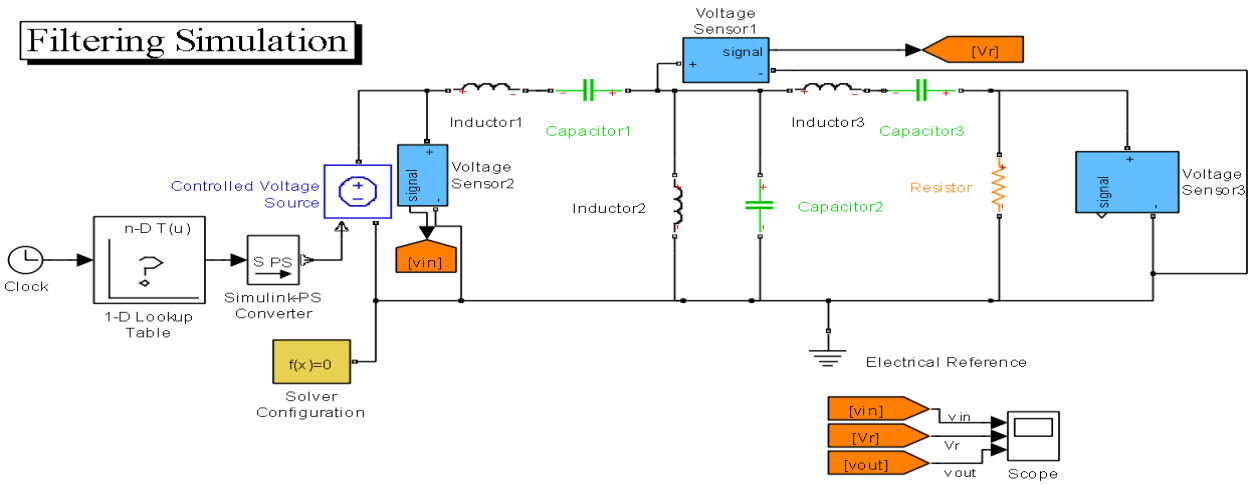

Figure 24: Matlab LC Filter Model

As can be seen the model is very similar to that of the Multisim only this uses a variable voltage input rather than multiple sinusoidal sources. The Lookup table supplies the varying ATP model voltages with time. The values of the inductors and capacitors were identical to the Multisim simulation as stated above. After many simulations the results were not quite as predicted. An investigation of the ATP output was done and the conclusion from it was that the time step of the ATP output was not periodic. The changes in time varied from 5us to 4.8us. Matlab was then coded to take in the entire dataset and linearly average the time step to 5us. These values were then utilized to simulate the LC filter. The result of the simulation is shown below.

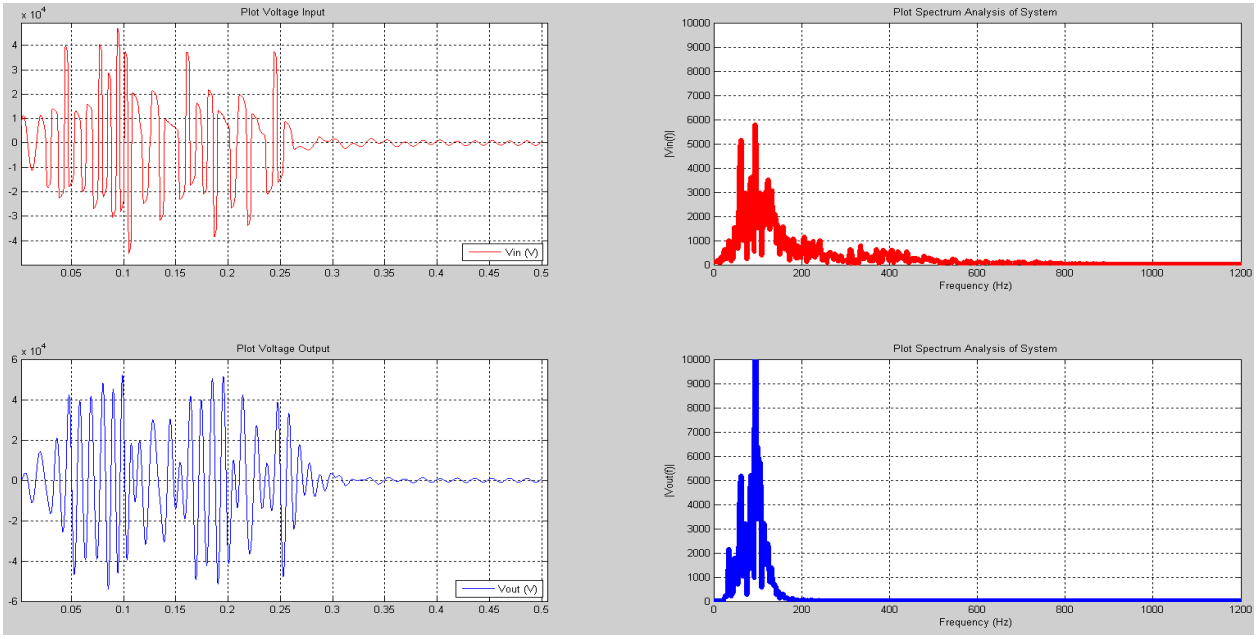

Figure 25: Matlab LC Filter Results

This result shows the complexities in the era of simulation packages. The upper left (red) plot is the original ATP voltage waveform re-simulated in Matlab. Red one of the right is the frequency spectrum analysis of the simulation. As can be seen there are multiple harmonics in the original wave. Also the original waveform was very noisy consisting of square wave like attributes. The filtered waveform (blue) takes the harmonics of the original and converts them to a sinusoidal voltage around the 100Hz frequency. This is not what was expected. It was expected to filter out all but the 60Hz component as was shown in the Multisim simulation. However, it can be seen that the filtered waveform is more sinusoidal and has fewer high frequency harmonics present.

Ideal Butterworth Filter

The T style LC filter was not very successful in suppressing the harmonics in the correct frequency band. It was determined that a test utilizing an ideal Butterworth filter should tested to see what an ideally created filter result would look like if it could be created. The figure below show the result of a Butterworth filter using a lower pass band of 50Hz, a higher pass band of 70Hz, and 3 orders of filtration. The model of the filter is as shown below:

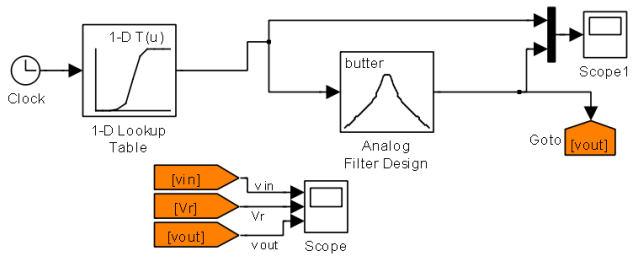

Figure 26: Matlab Ideal Butterworth Filter Model

This model completely negates any need for real filter components like resistors, inductors and capacitors. The resulting simulation of this is shown below:

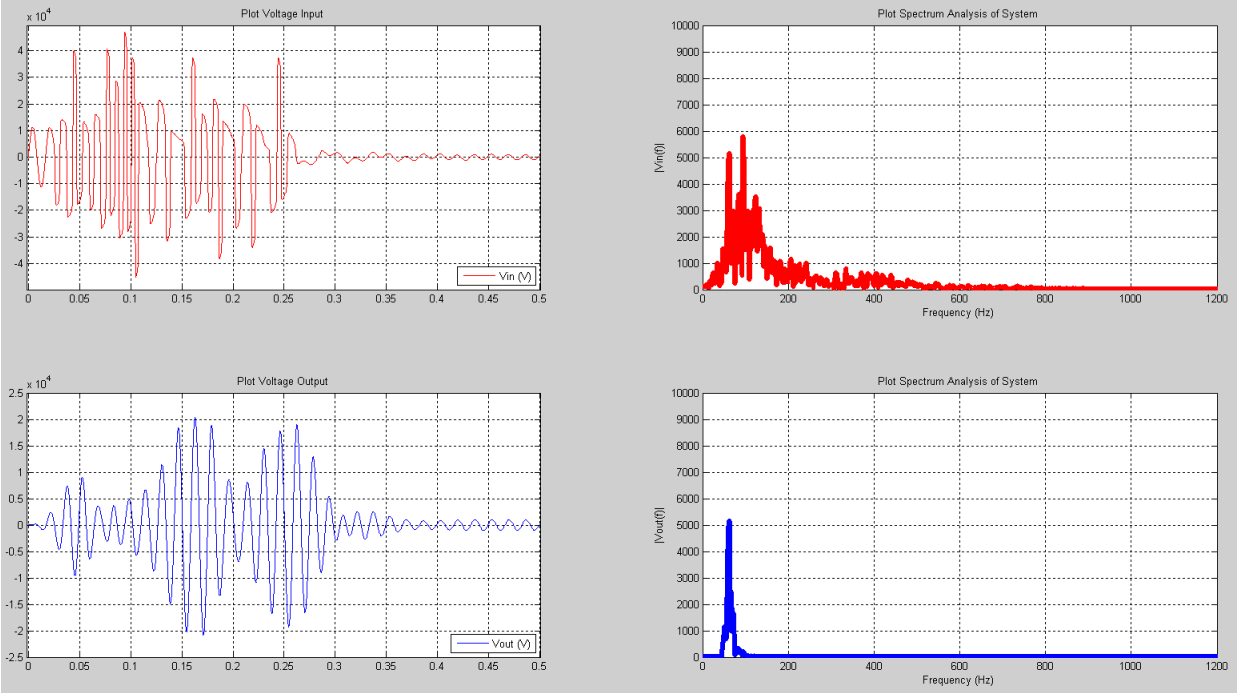

Figure 27: Matlab Ideal Butterworth Simulation Results

As can be seen the red is again the original waveform from ATP. The blue ideal Butterworth filter can be seen to reduce the peaks of the voltage spikes as well as correctly pass only the 60Hz component of the incoming waveform. From this it was decided to try and implement a new filter equation. This filter equation takes into account the varied peak phenomena in a bandpass filter and accounts for it using varying capacitor and inductor values. The implementation of the T-style filter stays the same as before so the Matlab model did not change. The value input for the inductors and capacitors however does, in accordance with the equations below.

$$L1 = L2 = \left(\frac{Zo}{\pi * (f2 - f1)}\right) \div 2$$

$$L2 = \frac{Zo * (f2 - f1)}{4 * \pi * f2 * f1}$$

$$C1 = C3 = \left(\frac{f2 - f1}{4 * \pi * f2 * f1 * Zo}\right) * 2$$

$$C2 = \frac{1}{(\pi * Zo * (f2 - f1))}$$

The value of Z_0 is equal to the resistive value used in the simulation (2350 Ohms). The value of F1 and F2 are equivalent to the cut off frequencies in hertz. L1, L2, L3 and C1, C2, C3 are the physical component values in Henries and Farads respectively. The frequency band used was from 50-70Hz. The resulting simulation is shown below.

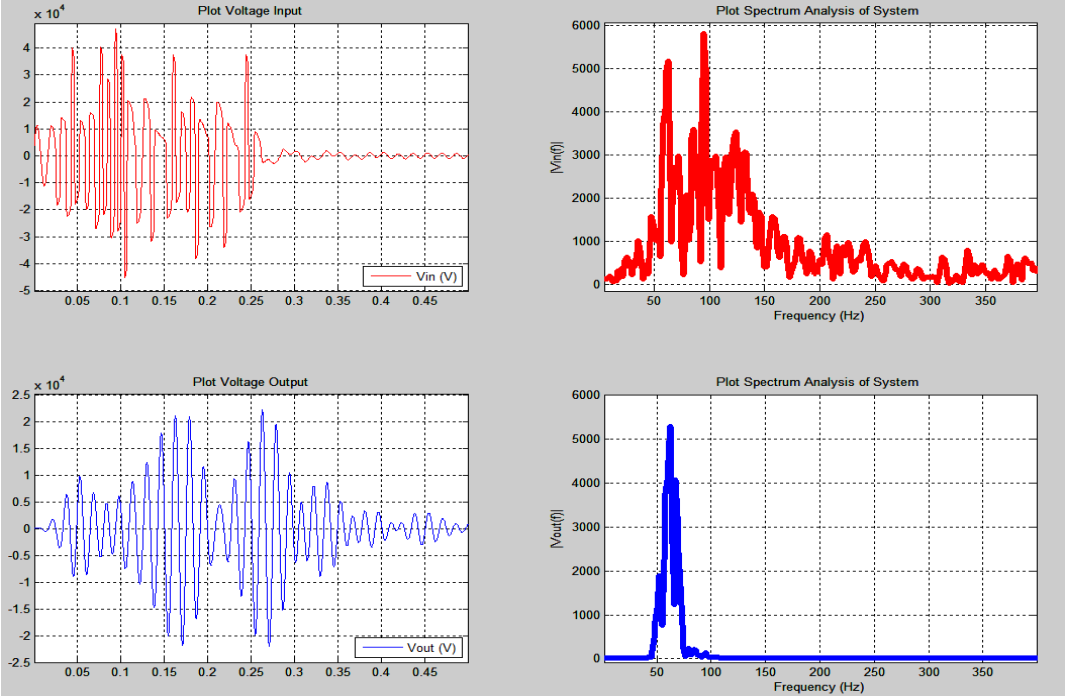

Figure 28: Secondary Equation Simulation Results

As can be seen this filter operates much more like anticipated. The new equations that shift the multiple order differential equations peaks closer together provide the wanted 60Hz component and eliminate the DC as well as higher components. It can also be noted that the voltage waveform is very sinusoidal and "clean" as well as having peaks about half that of the injected ferroresonant state with\out filtering. From this it can be concluded that a harmonic filter could be utilized to suppress the incoming harmonics that make ferroresonance so dangerous.

Other Mitigation Solutions

Although the harmonic content due to ferroresonance is mitigated using the filter solution, but still there does exist a high voltage magnitude on both the primary and secondary ends. There is still a risk to life and equipment presented by the fundamental component of voltage overshoot. Many physical solutions to this problem are prescribed in ref [6, 16] out of these two mitigating techniques have been implemented in this project and are mentioned below.

1. *Addition of Damping Resistance across the secondary winding.*

As discussed in most journal papers, a simple solution to suppress or prevent the occurrence of ferroresonance is by providing damping in the circuit. This can be achieved by addition of a wye connected resistor bank on the secondary.

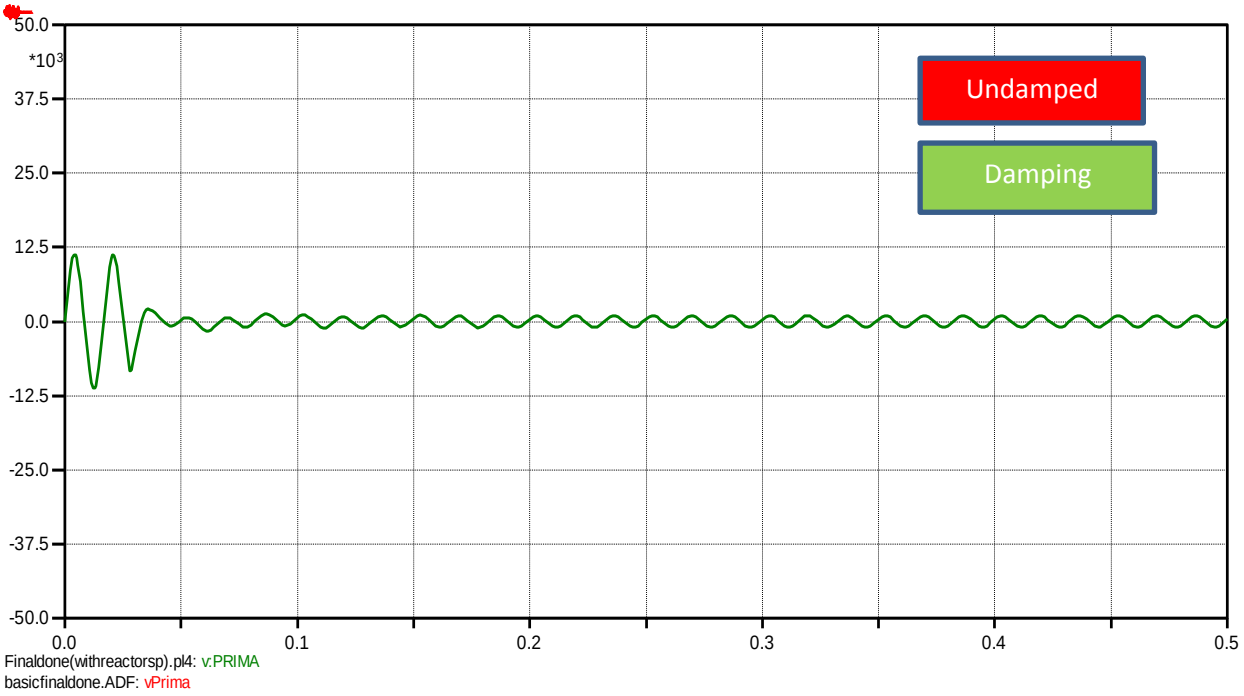

Figure 29: Addition of resistive damping circuit

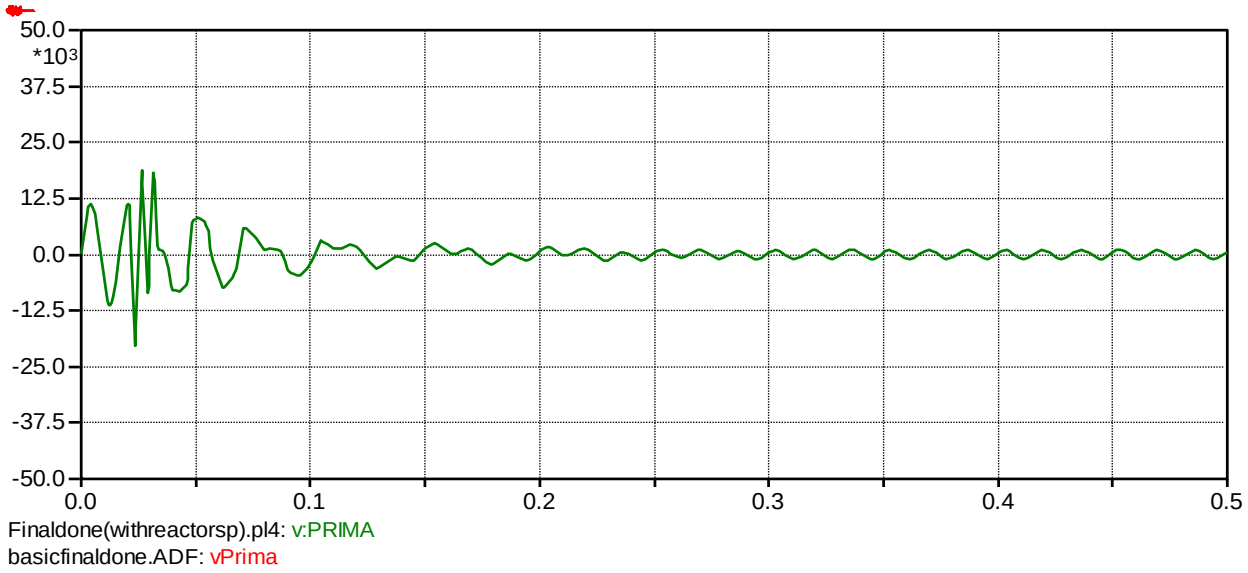

2. *Use of air-core reactor bank connected at the secondary*, though the author prescribes using one on the primary circuit, the addition of it on the secondary was implemented because of obvious reasons of low voltage rating. Care has to be taken when designing the inductor values and placement so as to not form an oscillatory circuit with the any other capacitive sources in our system.

Industry Solutions

Currently many manufacturers make harmonic filters for low, medium and high voltage applications. While medium and high voltage applications are less popular due to their expense they do exist. A company by the name of Arteche stocks low voltage (480V) low pass filters typically used for motor drive applications in industrial factories with high frequency harmonics. They also manufacture medium voltage (1kV-35kV) and high voltage (35kV and up) units that are custom tailored to the situation or objective. They manufacture both low pass and tuned harmonic filters. Another possibility is the utilization of active harmonics filters. Utilizing power electronics to inject current at certain times the harmonic can be offset. This type of system was not discussed here due to its lack of ability in medium voltage and up utility systems and are typically reserved for lower voltage industrial applications.

Currently ABB & KMB Systems provide commercial solutions for ferroresonance detection & suppression in instrument transformer. ABB module works on zero-sequence voltage threshold values generated on account of unbalance.

Also the practice of using temporary load banks when carrying out single phase switching operations on transformers is adopted all over.

Result

1. The proposed filter can be derived by making a compromise between the L & C values, physical limitations on their construction should be considered. A shunt nature of filter is advised so as to ground out the harmonic components.

2. Though the ferroresonance overvoltages have died down in the simulation either due to the systems natural damping characteristics or the inductance of the transformer falling out of saturation. In practice the case may not be the same. To test this, simulations with the addition of typical values of grading & surge capacitances were also carried out. The waveforms and results exhibited have been attached in Appendix C.

3. The output waveforms after suppression are restricted to manageable levels and the harmonics are prevented from travelling to the load end, avoiding stresses on equipment & enhancing safety of system.

Conclusion

The simulated low frequency transient phenomenon of ferroresonance was suppressed using an air core inductor bank connected to the secondary of the transformer. The contributing harmonics were filtered out using a LC *'T'* type Butterworth filter. The complexity of a ferroresonance circuit formation makes it difficult to be predicted. Thus, it is advisable to have back up suppression circuitry connected in the system. The filter so designed consumes zero active power and can be placed in the system not just for suppressing harmonics generated due to ferroresonance but also other transient events.

Future Work

1. A suggested filtering approach by Dr. Mork is creating a moving window non-recursive type filtering technique to deal with the harmonics.
2. Developing a standard technique to identify the onset of ferroresonance based on the harmonic content analysis & voltage overshoots duration.

References

[1] Swee Peng Ang, “Ferroresonance Simulation of Transmission Systems”, *Thesis, Faculty of Engineering and Physical Sciences, University of Manchester, 2010*.

[2] Greenwood Allan, “Electrical Transients in Power Systems”, *Wiley & Sons, 2nd Edition*.

[3] John Horak, “A review of Ferroresonance”, *Basler Electric Company*.

[4] Roy, M.; Roy, C.K., "Experiments on Ferroresonance at Various Line Conditions and Its Damping," *Power System Technology and IEEE Power India Conference, 2008. POWERCON 2008. Joint International Conference on*, vol., no., pp.1,8, 12-15 Oct. 2008. doi: 10.1109/ICPST.2008.4745305.

[5] Santoso Surya; Dugan C. Roger; Nedwick Peter, “Modeling Ferroresonance Phenomena in an Underground Distribution System”, *IPST conference, 2001*. http://www.ipst.org/techpapers/2001/ipst01paper034.pdf

[6] Escudero, M.V.; Dudurych, I.; Redfem, M., "Understanding ferroresonance," *Universities Power Engineering Conference, 2004. UPEC 2004. 39th International* , vol.3, no., pp.1262,1266 vol. 2, 8-8 Sept. 2004.

[7] Jacobson, D. A N; Swatek, D.R.; Mazur, R.W., "Mitigating potential transformer ferroresonance in a 230 kV converter station," *Transmission and Distribution Conference, 1996. Proceedings., 1996 IEEE* , vol., no., pp.269,275, 15-20 Sep 1996 doi: 10.1109/TDC.1996.545946.

[8] Jacobson, D. A N, "Examples of ferroresonance in a high voltage power system," *Power Engineering Society General Meeting, 2003, IEEE* , vol.2, no., pp.,1212 Vol. 2, 13-17 July 2003 doi: 10.1109/PES.2003.1270499.

[9] Mork, B. A., “Understanding and Dealing with Ferroresonance”, *Proceedings of Minnesota Power Systems Conference*, Minneapolis, MN, pp.6-1, November 7-9, 2006.

[10] Mysore, P.G.; Mork, B.A.; Bahirat, H.J., "Improved Application of Surge Capacitors for TRV Reduction When Clearing Capacitor Bank Faults," *Power Delivery, IEEE Transactions on* , vol.25, no.4, pp.2489,2495, Oct. 2010 doi: 10.1109/TPWRD.2010.2050605.

[11] Mokryani, G.; Haghifam, M.-R.; Latafat, H.; Aliparast, P.; Abdollahy, A., "Analysis of ferroresonance in a 20kV distribution network," *Power Electronics and Intelligent Transportation System (PEITS), 2009 2nd International Conference on* , vol.1, no., pp.31,35, 19-20 Dec. 2009 doi: 10.1109/PEITS.2009.5407008.

[12] Dugan, R.C., "Examples of ferroresonance in distribution," *Power Engineering Society General Meeting, 2003, IEEE* , vol.2, no., pp.,1215 Vol. 2, 13-17 July 2003 doi: 10.1109/PES.2003.1270500.

[13] Morgan, L.; Barcus, J.M.; Ihara, S., "Distribution series capacitor with high-energy varistor protection," *Power Delivery, IEEE Transactions on* , vol.8, no.3, pp.1413,1419, July 1993 doi: 10.1109/61.252668.

[14] Swift, G.W., "Power Transformer Core Behavior Under Transient Conditions," *Power Apparatus and Systems, IEEE Transactions on* , vol.PAS-90, no.5, pp.2206,2210, Sept. 1971 doi: 10.1109/TPAS.1971.293042.

[15] Hoidalen H K; Chiesa Nicola, "Modeling of nonlinear and hysteric iron-core inductors in ATP", http://www.elkraft.ntnu.no/~chiesa/Files/EEUG07_Chiesa.pdf.

[16] Ferracci Phillipe, "Ferroresonance", *Cahier Technique n^{o} 190*, March 1998, Groupe Schneider.

Appendix

A]

System physical data:

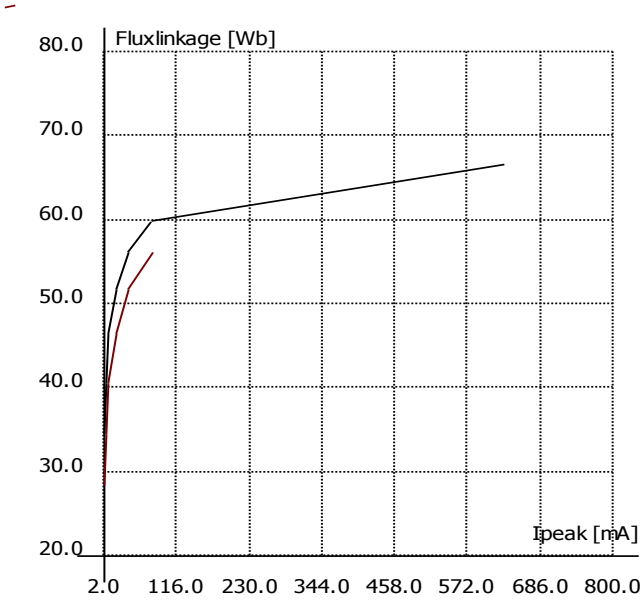

PVC triplex cables with cross-section of 35mm^2 and voltage class of 8.7/15 kV.

The cable electrical parameters are:

1. Positive sequence resistance: 0.6726_/km
2. Positive sequence reactance: 0.1793_/km
3. Zero sequence resistance: 1.6793_/km
4. Zero sequence reactance: 0.6332_/km
5. Capacitance: 0.2240 μF/km

2) 75kVA distribution transformer (Δ / Y)

a) No-load test (low-voltage)

1. Voltage: 220V
2. Current: 1.6%
3. Losses: 287W

b) Short-circuit test (high-voltage)

1. Losses: 1140W

2. Percentage impedance: 3.5%

c) Core data

1. Window height: 280mm

2. Window width: 115mm

3. Cross section area: 105.22cm2

4. Core material: M4 (0.27mm)

5. Diameter: 126mm

6. Leg length: 0.52m

7. Yoke length: 0.6m

d) Low-voltage winding

1. Internal diameter: 131mm

2. External diameter: 154mm

3. Coil conductor (copper): two axial and one radial 2x (7.5mm x 5mm)

4. Winding height: 254mm

e) High-voltage winding

1. Internal diameter: 176mm

2. External diameter: 218mm

3. Coil conductor: 0.65mm2

4. Winding height: 238mm.

Voltage (pu)	Current (%)	Losses (W)
0.701	0.22	85
0.81	0.448	131
0.907	0.843	193
1.00	1.6	287
1.10	2.979	420
1.209	6.061	650

Harmonic Content in fundamental mode of ferroresonance:

```
MC's PlotXY - Fourier chart(s).  Copying date: 27-04-2013
File Finaldone.pl4   Variable v:PRIMA [peak]
Initial Time: 0.48    Final Time: 0.5
Harm.    Amplitude       Phase
0        -58.522 0
1        813.49  -10.519
2        298.88  174.68
3        152.07  175.84
4        105.67  179.09
5        82.46   178.64
6        67.09   177.24
7        56.745  179.3
8        49.672  -179.87
9        43.814  178.57
10       39.188  179.07
11       35.693  -179.67
12       32.611  179.71
13       30.009  179.39
14       27.91   -179.89
15       25.987  -179.8
16       24.32   180
17       22.936  -179.84
18       21.617  -179.74
19       20.445  -179.61
20       19.465  -179.52
21       18.514  -179.62
22       17.643  -179.5
23       16.904  -179.25
24       16.189  -179.34
25       15.523  -179.37
26       14.944  -179.16
27       14.38   -179.09
28       13.855  -179.13
29       13.394  -179.06
30       12.938  -178.96

 THD=48.169%
```

Appendix B]

Frequency Sweep (Constant 2.44uF / 175kVAR @13.8kV)		
Frequency	Inductance (Henrys)	Capacitance (Farads)
60	2.886616171	2.43752300E-06
100	1.039181821	2.43752300E-06
500	0.041567273	2.43752300E-06
1000	0.010391818	2.43752300E-06
1500	0.004618586	2.43752300E-06
2000	0.002597955	2.43752300E-06

Frequency Sweep (Constant 2.44uF / 100kVAR @13.8kV)		
Frequency (Hz)	Inductance (Henrys)	Capacitance (Farads)
60	5.051577894	1.3928703974296E-06
100	1.818568042	1.3928703974296E-06
500	0.072742722	1.3928703974296E-06
1000	0.01818568	1.3928703974296E-06
1500	0.008082525	1.3928703974296E-06
2000	0.00454642	1.3928703974296E-06

Frequency Sweep (Constant 2.44uF / 50kVAR @13.8kV)		
Frequency	Inductance (Henrys)	Capacitance (Farads)
60	10.10315579	6.96435198714798E-07
100	3.637136083	6.96435198714798E-07
500	0.145485443	6.96435198714798E-07
1000	0.036371361	6.96435198714798E-07
1500	0.016165049	6.96435198714798E-07
2000	0.00909284	6.96435198714798E-07

```
%% Script Information
% EE5223
% Term Project
% Bandpass Filter Simulation
% Beau Baldwin
% April 25, 2013

%% Clear Workspace
clc          % Clears Command Window
close all    % Closes all figures
clear all    % Clear workspace

%% Define values

% Use Engineering Values
format short eng

% Parameters
R = 2350;          % Resistor  value (ohms)
```

```
Zo = R;
f2 = 70; %Hz
f1 = 50; %Hz

L11 = Zo/(pi*(f2-f1));

L22 = Zo*(f2-f1)/(4*pi*f2*f1);

C11 = (f2-f1)/(4*pi*f2*f1*Zo);

C22 = 1/(pi*Zo*(f2-f1));

C1 = C11*2;      % Capacitor values (Farads)
C2 = C22;
C3 = C11*2;

L1 = L11/2;        % Inductance values (Henries)
L2 = L22;
L3 = L11/2;
```

```
C1 = 2.43752300e-06;      % Capacitor values (Farads)
C2 = 2.43752300e-06;
C3 = 2.43752300e-06;

L1 = 2.886616171;        % Inductance values (Henries)
L2 = 2.886616171;
L3 = 2.886616171;


% Create Time Data (Time_Step)
dT = 0.000005;
```

```
%% Open Data File

Vprima = xlsread('Final.xlsx','B2:B100002');
time = xlsread('Final.xlsx','A2:A100002');
n=100001;
t1=0;
t2=.5;
ti = linspace(t1,t2,n);
voltt = interp1(time,Vprima,ti);




%% Open Model
model='EE2112_Spr2013_L25_LowPassFilter_wLookup_MDL.mdl';
open(model)

%% Simulation
tstop = .5;   % simulation time

% Simulation Call
 sim(model, [0,tstop])

 %% Plot Results
% Extract the data from Structure
% This save the data to a more "userable" name
time = ScopeData.time;
Vin = ScopeData.signals(1,1).values;
Vr = ScopeData.signals(1,2).values;
Vc = ScopeData.signals(1,3).values;

%% FFT Calculation
% Used below website as basis for FFT plot
% website http://www.mathworks.com/help/matlab/ref/fft.html;jsessionid=5456bf2e20e5361e232fde251a43
y1=Vin;
y2=Vc;
Fs = 1/dT;              % Sampling frequency
T = dT;                % Sample time
L = length(y2);          % Length of signal
t = (0:L-1)*T;          % Time vector

NFFT = 2^nextpow2(L);     % Next power of 2 from length of y
Y1 = fft(y1,NFFT)/L;
Y2 = fft(y2,NFFT)/L;
f = Fs/2*linspace(0,1,NFFT/2+1);

%% Plot Data
figure_handle = figure;


% Define Subplot Steps
```

```
subplot(2,2,1)
    plot(time,Vin,'r')
    grid on
    plottitle = sprintf('%s', 'Plot Voltage Input');
    title(plottitle)
    legend('Vin (V)','Location','SouthEast')

% Define Subplot Steps
subplot(2,2,3)
    plot(time,Vc,'b')
    grid on
    plottitle = sprintf('%s', 'Plot Voltage Output');
    title(plottitle)
    legend('Vout (V)','Location','SouthEast')


% find all axes handle of type 'axes' and empty tag
all_ha = findobj( figure_handle, 'type', 'axes', 'tag', '' );
linkaxes( all_ha, 'x' );



% Plot single-sided amplitude spectrum.
subplot(2,2,2)
    plot(f,2*abs(Y1(1:NFFT/2+1)),'r','LineWidth',5)
    title('Single-Sided Amplitude Spectrum of y(t)')
    axis([0 1200 0 10000])
    xlabel('Frequency (Hz)')
    ylabel('|Vin(f)|')
    grid on
    plottitle = sprintf('%s%s', 'Plot Spectrum Analysis ','of System ');
    title(plottitle)

subplot(2,2,4)
    plot(f,2*abs(Y2(1:NFFT/2+1)),'b','LineWidth',5)
    title('Single-Sided Amplitude Spectrum of y(t)')
    axis([0 1200 0 10000])
    xlabel('Frequency (Hz)')
    ylabel('|Vout(f)|')
    grid on
    plottitle = sprintf('%s%s', 'Plot Spectrum Analysis ','of System ');
    title(plottitle)
```

Appendix C]

Grading and Surge Capacitors

In order to look into the effects of circuit capacitance on ferroresonance modes, a sensitivity analysis was carried out tweaking the absolute values of the grading and surge capacitances that can be present in this particular system.

For a 13.8 kV system the practical values of grading capacitors & surge capacitors for the breaker where obtained from references [16, 17, 18].

C_{surge} = 0.25uF

$C_{grading}$ = 200pF

Grading Capacitors: Capacitors added across the circuit breaker interrupters to distribute voltage during opening of a 3phase separated breaker.

Surge Capacitors: Surge capacitors are added on either sides of a breaker in order to control both the Transient recovery voltage (TRV) and rate of rise of recovery voltage (RRRV) that typically occur in the presence of current limiting reactors which can result in high RRRV after breaking high short circuit currents. Their values are estimated based on the CB's interrupting current ratings and reactor size [10].

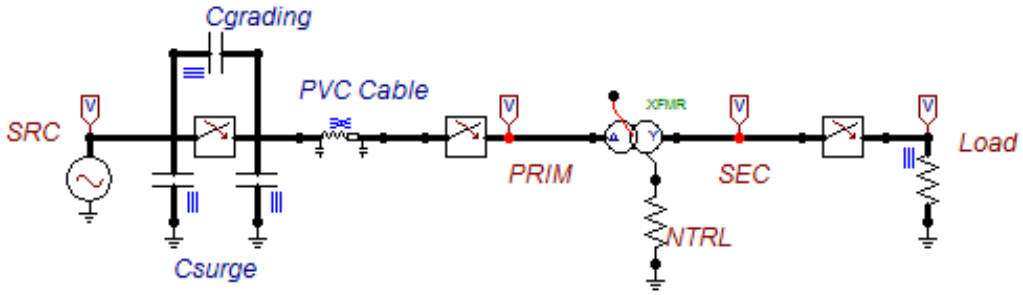

Figure 30: Simulation Model with Capacitors

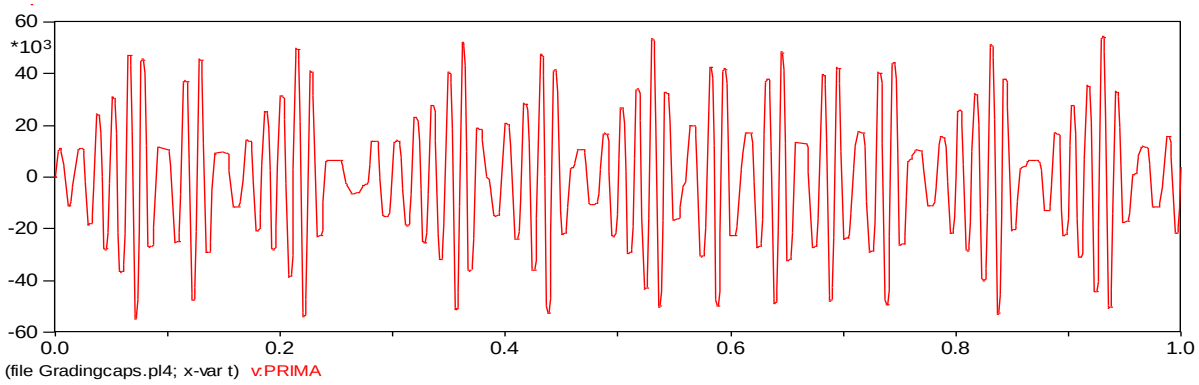

Figure 31: Response of System with Grading & Surge Caps (Over-Voltages Continues to Propagate)

As can be seen the response of the system is simply delayed compared to the circuit with no added grading & surge capacitors shown below.

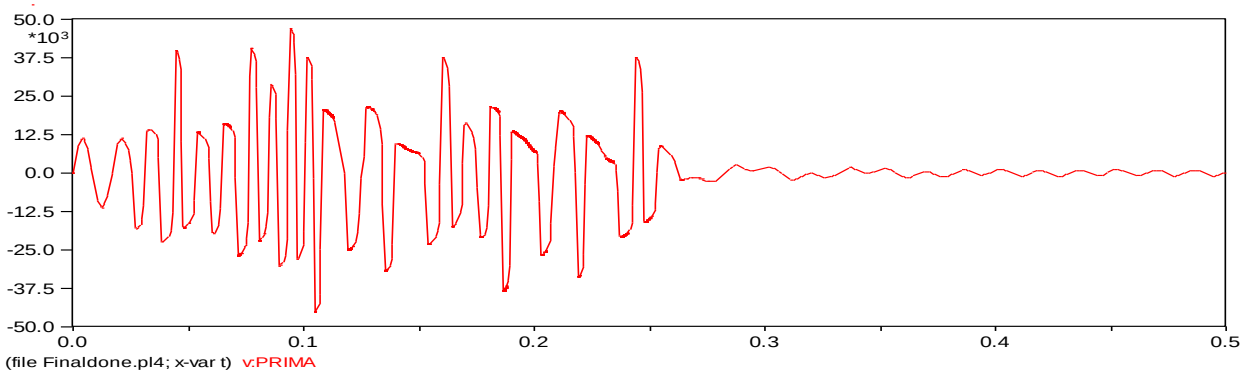

Figure 32: Response of The System w/Out Grading & Surge Caps (Overvoltages damp down)

Below is the Fourier analysis of the voltage waveform with the added grading and surge capacitors. As can be seen the first harmonic is again the primary component with the following harmonic orders following the fundamental mode of ferroresonance.

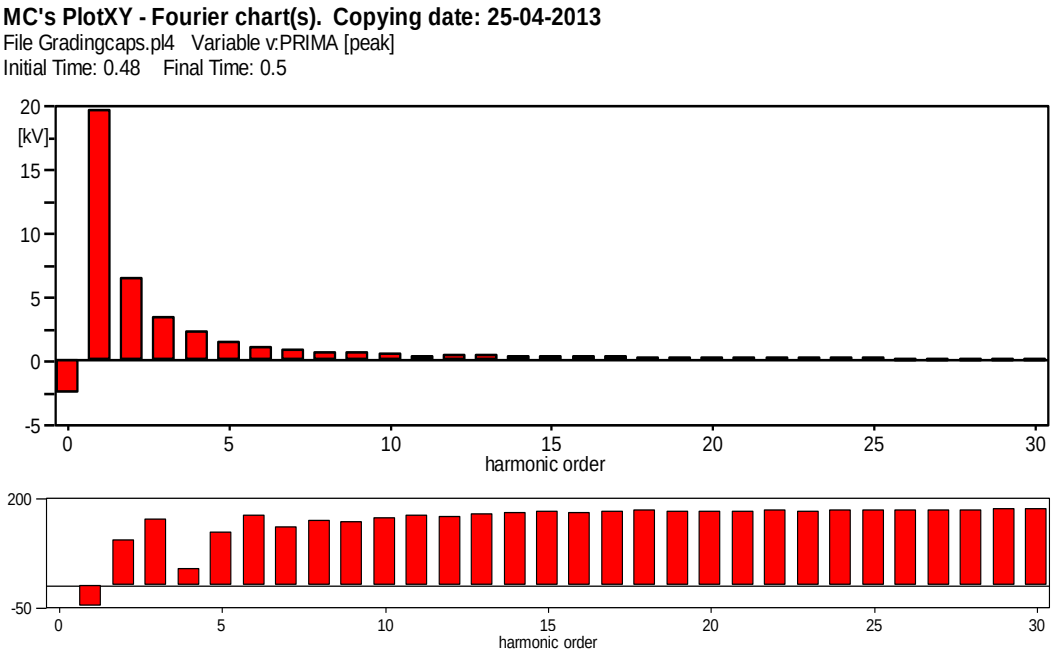

Figure 33: Fourier Analysis with Added Capacitance

The same suppression techniques have been implemented on the modified circuit resulting in the following waveforms.

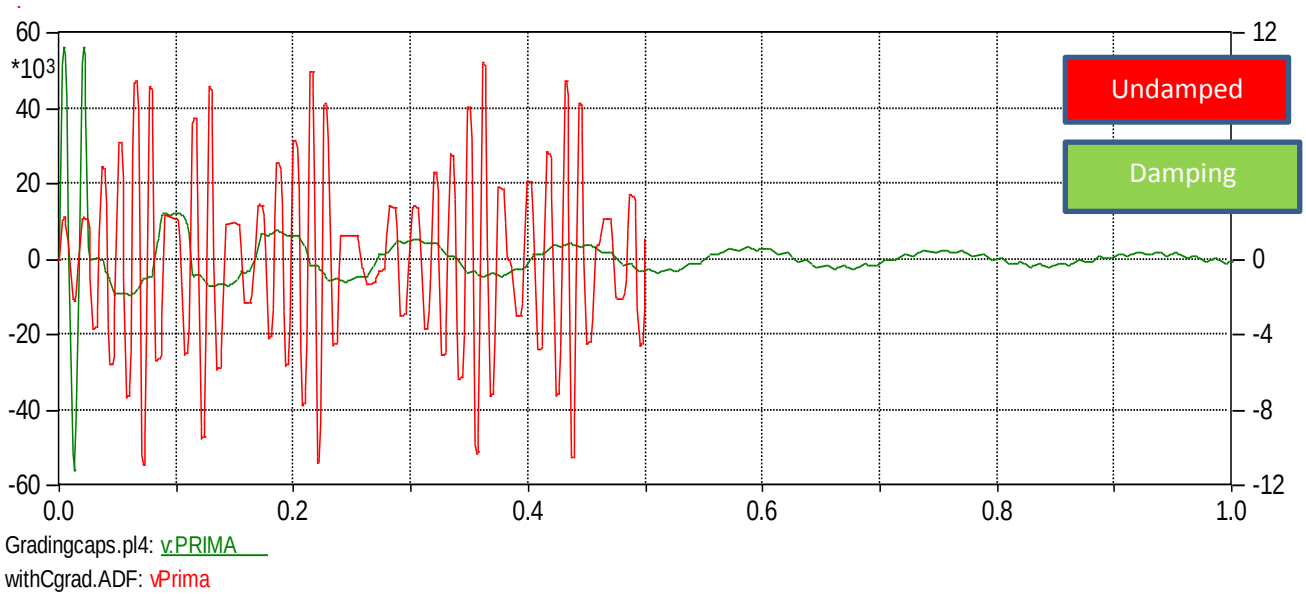

Figure 34: Suppressed using 300 ohms resistance bank at primary

There can be harmonics noticed since a filter was not incorporated in the circuit.

File Gradingcaps.pl4 Variable v:PRIMA [peak]

Initial Time: 0.48 Final Time: 0.5 THD=41.315%

Harm.	Amplitude	Phase
0	-2471	0
1	19605	-47.915
2	6450.1	104.22
3	3423.8	149.67
4	2253.1	36.963
5	1477.9	121.67
6	1120.4	160.7
7	899.72	132.9
8	646.38	148.16
9	646.12	143.95
10	602.92	153.65
11	405.23	158.91
12	480.09	156.1
13	465.17	163.59
14	399	165.28
15	374.43	168.35
16	332.3	164.91
17	309.51	169.63
18	278.37	171.46
19	274.93	169.51
20	252.2	169.04
21	254.81	169.32
22	231.43	171.42
23	216.99	169.12
24	214.4	172.07
25	205.53	171.72
26	197.45	172.11
27	190.4	171.98
28	187.72	172.6
29	178.13	173.62
30	171.88	174.45